International Journal of Applied Engineering Research ISSN 0973-4562 Volume 12, Number 21 (2017) pp. 10951-10957

A Multi-Input DC-DC Converter with Effective Charging of Energy Storage Source

Kushal A. Kanhav[1]
Assistant Professor, Department of Electrical Engineering
St. Vincent Pallotti College of Engineering and Technology Nagpur
Gavsi Manapur, Wardha Road, Nagpur, Maharashtra- 441108, India.
Orcid Id: 0000-0001-7793-8783

Madhuri A. Chaudhari[2]
Associate Professor, Department of Electrical Engineering,
Visvesvaraya National Institute of Technology Nagpur
South Ambazari Road, Nagpur, Maharashtra-440010, India.
Orcid Id: 0000-0001-5500-6723

Abstract

In hybrid and renewable energy system, multiple-input converter is the best choice to integrate various input sources for supplying power to the load. In this paper, a multi-input DC-DC converter having ability to transfer energy from one of the sources to the energy storage source is presented. This feature results in improved reliability. In addition to this, energy sources having distinct voltage levels and characteristics can be interfaced to the converter. It also provides isolation between source and load without using transformer. The load voltage is regulated irrespective of the dynamics at the input and output of the converter. The operating condition decides the working modes of the converter i.e. buck, boost and buck-boost mode. A low power laboratory prototype is developed for experimental study of the converter. The analysis, design, simulation and experimental results of the converter proved that the converter is suitable for hybrid electric or green energy system applications.

Keywords: Multiple-input converter, dc-dc converter, hybrid electrical system, renewable energy system

INTRODUCTION

In hybrid electric vehicles (HEVs), fuel cell vehicles (FCVs), renewable energy systems (RESs) and in many industrial applications, the demand of high-power, high-frequency and high-density dc-dc converters is increasing day by day. The applications and advantages of multiple-input converters (MICs) are widely discussed in the literature (Danyali 2014; Onwuchekwa 2012; Jiang 2011; Kumar 2013; Liu 2014; Dusmez 2016; Li 2015). [1-7]. MICs are preferred in applications, such as HEV, FCVs and RESs, as it is cheaper, uses less components, provides higher power density, and gives better performance. Hence, MICs are sometimes called as power/energy management converter.

RESs are increasingly becoming popular for generation of electricity due to limited supply of fossil fuels and the problems of environmental pollution caused by them. Solar photovoltaic (PV) systems are one of the best choices for electrification in the areas where the electric network does not exist. The main drawback of the solar PV systems is its intermittent nature. Therefore; solar PV systems require an energy storage component, which is normally realized by utilizing battery stacks (Sechilariu 2013) [8]. An isolated dc/dc converter for PV systems is discussed in (Zeng 2014) [9]. Different MIC topologies proposed by the research community mainly focus on non-isolated and isolated structures (Veerachary 2008; Yuan 2013; Wu 2015; Ahmadi 2012) [10-13].

The plug-in electric vehicles (PEVs) charging strategies are discussed in (Zheng 2014 and Hong 2015) [14, 15]. Thus, HEVs/FCVs/PEVs have encouraged the development of dc-dc converters having enhanced and effective charging techniques. The batteries and ultracapacitors (UCs) are the most common energy storage mechanisms used to hybridize energy systems. However, the high specific power of UCs is the major reason of them being used as an intermediate energy storage unit. The mathematical model is proposed for stability analysis of an integrated DC distribution power system for PEVs in (Tabari 2014) [16].

This paper aims to propose a MIC which has the capability to transfer energy from one of the sources to the energy storage source (ESS) with improved reliability. Following are the features of the proposed MIC: ability to interface asymmetrical sources; capability to transfer energy from one of the sources to the energy storage source (ESS) with output voltage control; enhance utilization of the MIC; less part count; enhanced charging of ESS; improved reliability in view of power supplied to the load; sources and the load are isolated without using transformer; and simple control.

Operation of the proposed MIC

The proposed MIC is shown in Figure 1. Two voltage sources V_1 and V_2 having dissimilar characteristics are connected to energize inductor L. A DC link capacitor C is connected across load, which provides power to the load during charging time of L. Load is isolated from the source during the operation of the MIC. Turn ON and OFF time of the switches is controlled by suitable application of pulse width modulated (PWM) signals at switching frequency, f_s. The load voltage is controlled by regulating the switching time of the switches. Load voltage and current (V_o,i_o), inductor voltage (V_L), inductor current (i_L), capacitor current (i_c), switch currents (i_1, i_2 and i_3), sources V_1 and V_2 are as shown in Figure 1.

Body diode of switches S_2, S_3 is D_2, D_3 respectively. Duty ratio of switches S_1, S_2, S_3 is d_1, d_2, d_3 respectively. Source V_1 is solar PV module and V_2 is ESS. Figure 2 shows operating states of the proposed MIC for $V_1 > V_2$, which are summarized in Table 1.

Gate pulse is given to switch S_3 if V_2 drop below specified value. The reliability of power flow from source to load is improved in state 4. In this state, S_3 is turned ON during the conduction period of S_1. Thus, converter recharges or maintains voltage of ESS V_2, provided $V_1 > V_2$ and $d_3 \leq d_1$. The direction of flow of current i_3 and i_2 get reversed, as it flows through S_3 and D_2 respectively. The voltage source V_1 charges source V_2 and inductor L. Load current is supplied by C, $i_o = i_c$ as shown in Figure 2(d). Thus, charging of V_2 takes place in this state.

The sequence of working states depends on status of the sources, load dynamics and control scheme. In this topology dual voltage sources with dissimilar voltage levels provides power to the load independently. Hence, output voltage can have different levels. Therefore, design of passive elements plays an important part in the load voltage stabilization and minimization of ripple in output current. The voltage levels and characteristics of sources V_1 and V_2 may be distinct hence, during the operation of MIC simultaneous conduction of S_1 and S_2 is avoided.

Gate signal of switches S_1, S_2 and S_3 are as shown in Figure 3. T_S is time period for one complete switching cycle of gate pulse. Inductor voltage (V_L), inductor current (i_L), switch current (i_3) when S_3 is in OFF state and capacitor current (i_c) for all working states of the MIC over a single switching period is as shown in Figure 4. The inductor current i_L is designed to be continuous. Losses due to switching and resistive drop across passive elements are neglected. The average value of V_o considering non-idealities is given in (1). V_o is obtained by applying KCL at node A and KVL in loop L1, L2 and L3 respectively as seen in the Figure 2(a), 2(b) and 2(c) for one complete switching cycle of gate pulse.

$$V_o = \frac{A\{[V_1 d_1 + (V_2 - V_{D3})d_2]\} - [A^2(V_{D3} + V_D)]}{\frac{r_l + R_D(d_1 + d_2)}{R} + A^2} \quad (1)$$

where; $A = (1 - d_1 - d_2)$; V_{D3} and V_D: Voltage drop of body diode of switch S_3 and diode D respectively;

R_D : ON state resistance of MOSFET, R: load resistance, r_l and r_c: internal series resistance of L and C respectively.

The average value of V_o for ideal circuit elements is obtained by putting $V_{D3} = V_D = R_D = r_l = 0$ in (1). Thus,

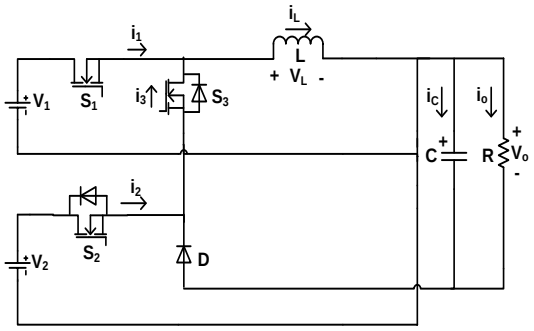

Figure 1: Circuit diagram of the proposed MIC

Table 1: Operating states of the proposed MIC ($V_1 > V_2$)

State	Active source	Switch ON state	V_L	L status	V_2 status	i_o status
1	V_2	S_2,D_3	V_2	chg	dchg	$-i_c$
2	V_1	S_1	V_1	chg	Nchg	$-i_c$
3	None	D_3,D	$-V_o$	dchg	Nchg	i_L-i_c
4	V_1	S_1,S_3, D_2	V_1	chg	chg	$-i_c$

chg-charging, dchg-discharging, Nchg-No charging

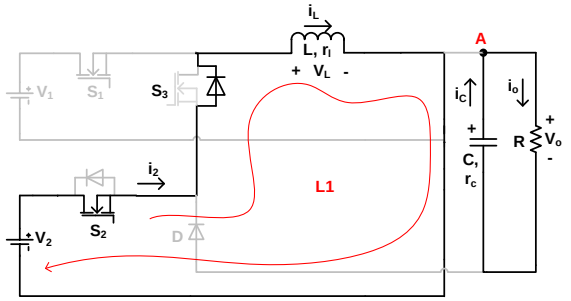

(a)

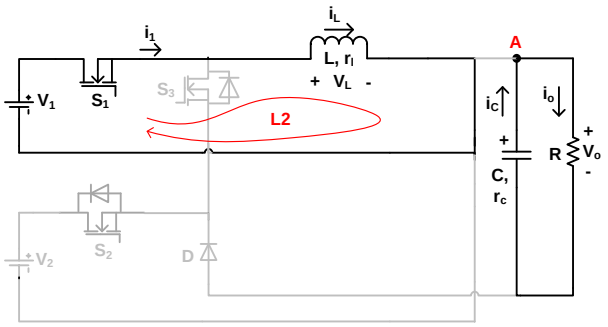

(b)

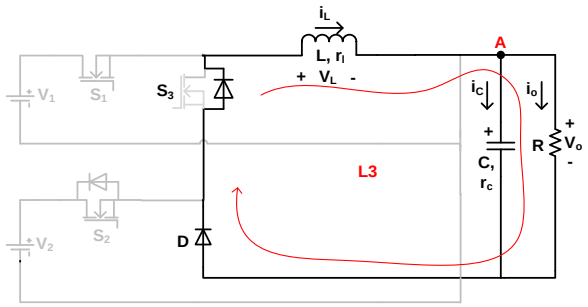

(c)

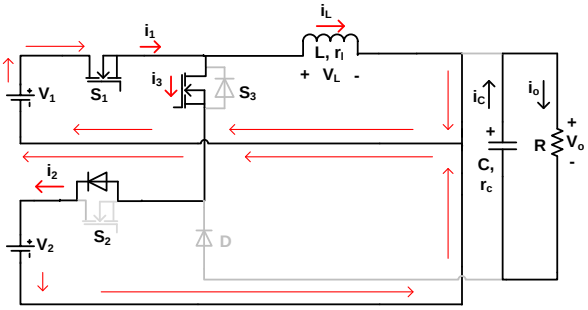

(d)

Figure 2: Operating circuits of the proposed MIC ($V_1 > V_2$): (a) State 1. Charging of L by V_2, (b) State 2. Charging of L by V_1, (c) State 3. Charging of C by L, (d) State 4. Charging of V_2 and L by V_1

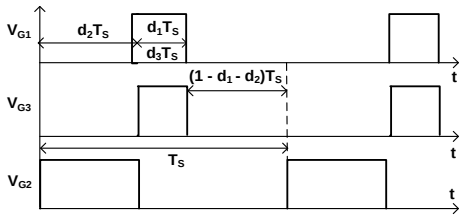

Figure 3: Switching signals ($d_3 = d_1$)

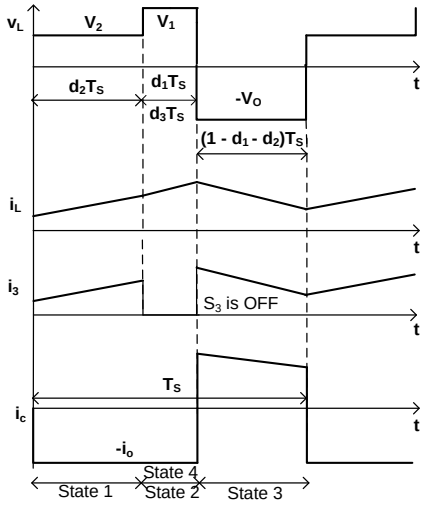

Figure 4: V_L, i_L, i_3 and i_c waveform

$$V_o = \frac{V_1 d_1 + V_2 d_2}{(1 - d_1 - d_2)} \quad (2)$$

The specified inductor current ripple (Δi_L) and output voltage ripple (Δv_c) gives the value of L and C which is calculated by using following expressions:

$$\Delta i_L = \frac{V_o(1 - d_1 - d_2)}{L f_s} \quad \text{and} \quad \Delta v_c = \frac{V_o(d_1 + d_2)}{RC f_s} \quad (3)$$

A comparison of the proposed MIC with the existing work is shown in Table 2. The MIC has the advantage in most of the features while it is comparable in remaining features with respect to number of ports. It has the ability to transfer energy effectively from one of the sources to the ESS with less number of switches in the energy transfer path is the merit of the proposed MIC. Thus, ESS can be charged simultaneously along with the inductor during the operation of the MIC leads to enhanced utilization of the proposed MIC.

Control strategies for the proposed MIC

This section proposes control strategy for the MIC operation with improved reliability. The controllers are designed such that, appropriate mode of MIC operation is selected as per the availability of sources and the load demand.

Output voltage is regulated by appropriate application of gate pulse to the switches which enhances MICs performance. The sequence of operating states can be changed by appropriate generation of gate pulses. Control of MIC is as shown in Figure 5. Gate signal of switches S_1, S_2, S_3 are V_{G1}, V_{G2} and V_{G3} respectively. S_1 and S_3 are controlled to achieve charging of ESS V_2 as per the requirement. The magnitude of load voltage is controlled by regulating the duty ratio d_1 and d_2.

Proportional and Integral controllers are used for current and voltage control. The load voltage (V_o), is sensed and processed to generate programmed current reference, which is further scaled to get current reference i_{1ref}.

Switch current (i_1), is sensed and processed to generate the gate pulses required for switch S_1, which forms a current loop of the MIC as shown in Figure 5(a). The gate pulses required for switch S_2, which forms a voltage loop of the MIC is generated as shown in Figure 5(b). Voltage sensors and current sensor are used to sense output voltage (V_o) and switch current (i_1). Thus, the sensed voltage and current are compared with reference voltage and current, it is then applied to the respective controller. The PWM control technique is used to provide control actions so as to regulate the output voltage of the MIC.

The function of the controller is to generate switching pulses for the connected sources which decides the quantity of power supplied by each source. The average value of output current I_o is a function of average value of input currents I_1 and I_2 i.e. I_o belongs to I_1 and I_2.

Table 2: Comparison of the proposed MIC

Topology	N_P	N_S	N_D	N_T	N_L	N_C	*OM*	*I*	N_W	*ET*
Lalit K [4]	3	3	3	6	1	1	b, B, b-B	YES	0	NO
Liu F [5]	3	4	2	6	2	2	B	YES	3	NO
Dusmez S [6]	3	4	8	12	3	3	B	YES	2	NO
Li W [7]	3	4	4	8	1	2	b-B	YES	2#	NO
Ahmadi R [13]	3	8	1	9	1	1	b, b-B	NO	0	NO
Proposed MIC	3	2	2	4	1	1	b, B, b-B	YES	0	**YES**

N_P: no. of ports, N_S: no. of switches, N_D: no. of diodes, N_T: total No. of switches and diodes, N_L: no. of inductors, N_C: no. of capacitors, *OM*: operating modes (*B*: boost, *b*: buck, *b-B*: buck-boost), *I*: isolation between sources and load, N_W: no. of transformer windings, #: winding-cross-coupled inductors (WCCIs), *ET*: Energy transfer from one source to another.

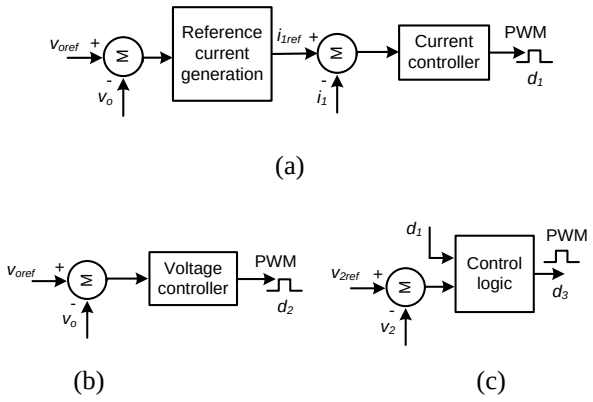

(a)

(b) (c)

Figure 5: Control of MIC: (a) Generation of V_{G1},
(b) Generation of V_{G2},
(c) Generation of V_{G3}

Hence, the controller decides the supplying source and the quantity of power drawn from it. Therefore, on the basis of load requirement and operating conditions suitable control signals are generated.

Charging of source V_2

Source voltage V_2 is monitored continuously with the help of a voltage sensor. As soon as the terminal voltage drops below specified value, the control logic generates gate pulse for switch S_3 during the ON time of switch S_1. Thus, charging path for source V_2 is completed through V_1 as shown in Figure 2(d). Charging of V_2 is stopped when its terminal voltage becomes equal to its rated value by making S_3 OFF. Thus, charging operation of V_2 is controlled by controlling the duty cycle of S_3 in synchronization with S_1 as shown in the Figure 5(c). Switching signal of S_1 and S_3 decides the charging of source V_2. Source V_2 can supply power to the load during the OFF time of S_1 if terminal voltage of V_2 is greater than or equal to 50% of its rated value. The voltage level of source V_2 along with output voltage V_o is regulated during MIC operation.

RESULTS AND DISCUSSIONS

Simulation results

To verify theoretical performance of the MIC, simulations are carried out with non-idealities using PSIM software, under different steady and transient conditions.

Table 3: Simulation parameters

V_1 (V)	V_2 (V)	f_s (KHz)	L (µH)	C (µF)	$r_l = r_c$ (Ω)	R (Ω)	V_o (V)
24	12	15	230	1000	0.05	10	24

R_D = 0.036 Ω and V_{D3} = V_D 1.2 V.

The simulation results for CCM operation have been analyzed under steady and dynamic conditions. For testing the performance of the MIC, different PWM gate signals are applied. Simulation results of gate voltage (V_{G1}, V_{G2}), inductor voltage and current (V_L, i_L), source voltage (V_2), output voltage and current (V_o, i_o) for various operating conditions with different combination of duty cycles are shown in the Figure 6. The open loop operation of the MIC in boost, buck-boost and buck mode is shown in Figure 6(a), (b) and (c) respectively, when S_3 is in OFF state.

Solar power is generally used as one of the sources in hybrid power system. The healthy source supplies power to the load if other source is cut-off, thereby improving the reliability of the MIC. The reliability and power transfer capability is improved by using solar-battery/UC hybrid system. V_1 is solar source, whereas V_2 is ESS. The power-voltage (P-V) and current-voltage (I-V) characteristics of solar source depend on various parameters such as operating temperature, insolation level, connected load, etc. Figure 6(d) and (e) shows close loop operation of the MIC. The charging of the source V_2 is achieved by turning ON S_3 as shown in the Figure 6(d) and (e), thereby validating the charging capability of the MIC.

From Figure 6(d) it is observed that when V_2 is charging output voltage V_o is regulated at 24 V before and after change in loading conditions. The rate of charging of V_2 increases after decrease in loading, as source V_1 (solar) can supply more current to charge V_2 due to decrease in load demand. Similarly, from Figure 6(e) it is observed that the load voltage V_o is regulated at 24 V before and after change in loading conditions. But; after increase in loading, V_2 supplies more current to satisfy the load demand. Thus, discharging rate of V_2 is more as compared to charging due to increase in loading. Output voltage V_o is regulated at 24 V for different dynamic conditions. The response of the converter is satisfactory during steady and dynamic conditions. Thus, simulation results validate the theoretical analysis.

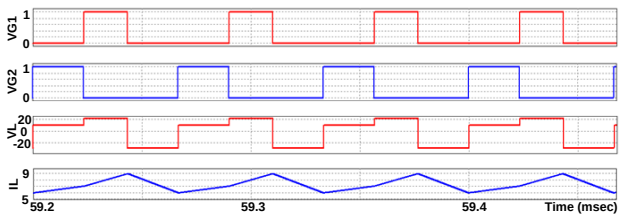

(a)

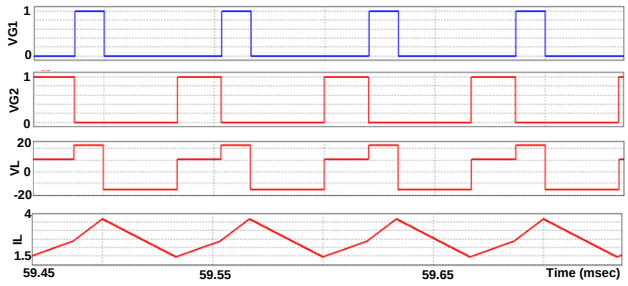

(b)

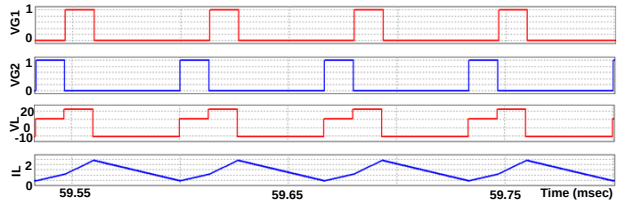

(c)

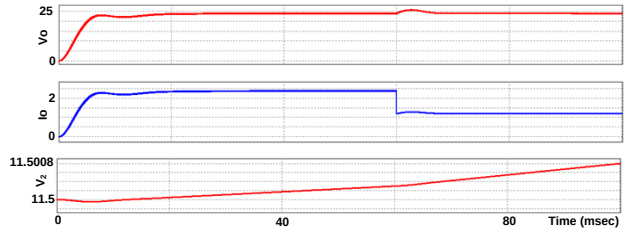

(d)

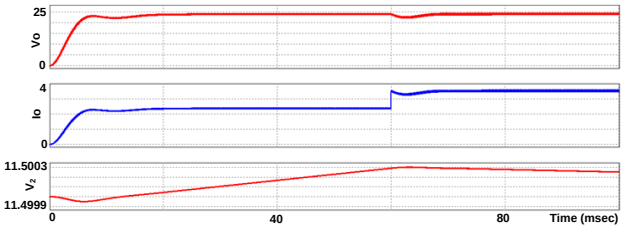

(e)

Figure 6: Simulation results: (a) Gate signal of S_1 and S_2; inductor voltage and current (d_1=0.3, d_2=0.35) (b) Gate signal of S_1 and S_2; inductor voltage and current (d_1=0.2, d_2=0.3), (c) Gate signal of S_1 and S_2; inductor voltage and current (d_1=d_2=0.2), (d) Output voltage and current; source voltage V_2 during step change (decrease) in loading by 50%, (e) Output voltage and current; source voltage V_2 during step change (increase) in loading by 50%

EXPERIMENTAL RESULTS

A low power laboratory prototype is developed for experimental realization of the proposed MIC as shown in Figure 7. A solar PV panel is installed over the rooftop of the laboratory. The MOSFETs IRFP 150N and diode MUR 1560 G are used as controlling switches in the power circuit. The MIC 4425 is used to drive the MOSFETs. The digital storage oscilloscope TPS 2024B; current probe A 622 and voltage probe Tek P5122 are used for measuring current and voltage. Current transducer LA 25-P and voltage transducer LV 20-P from LEM are used for sensing current and voltage respectively. The control system for the generation of gate signals at 15 KHz is implemented using dsPIC33EP256MC202, digital signal controller from Microchip. The on chip analog to digital converter (ADC) is programmed which is required for the digital control of the MIC. Source V_2 is Maxwell Technologies UC bank of 500 F, 16.2 V, consisting of six BCAP 3000 F, 2.7 V UCs connected in series. The value of L and C is 230 µH and 1000 µF respectively. Experimental results of gate voltage (V_{G1}, V_{G2}), inductor voltage and current (V_L, i_L), source voltage (V_2), output voltage (V_o) and current (i_3) in different modes of operation for various operating conditions are discussed below.

The operation of the MIC under various working conditions is shown in Figure 8. Figure 8(a) demonstrate converter operation in buck-boost ($V_2 < V_o < V_1$) mode respectively, when S_3 is in OFF state. Current i_3 flows in positive direction which indicates NO charging of ESS.

This shows that proposed MIC operates in buck, boost, buck-boost mode for output voltage regulation, depending on the availability of input sources. Figure 8(a) show waveforms of MIC for V_o = 24 V, when V_1 = 24 V, V_2 = 12 V and S_3 in OFF state. Thus, Figure 8(a) validates theoretical and simulation performance of the MIC. Rate of charging of inductor depends on magnitude of V_1 and V_2 whereas discharging rate depends on V_o which is clearly observed from i_L waveform.

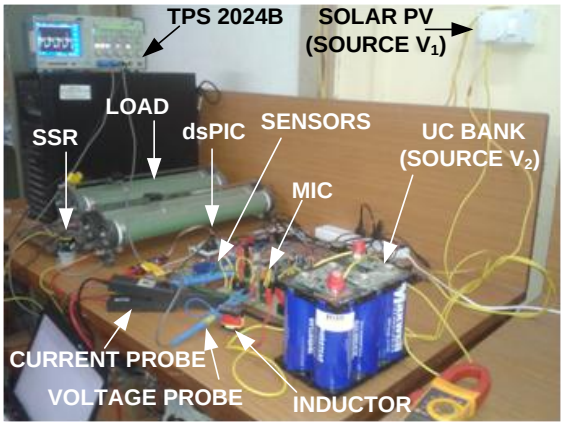

Figure 7. Laboratory setup of MIC

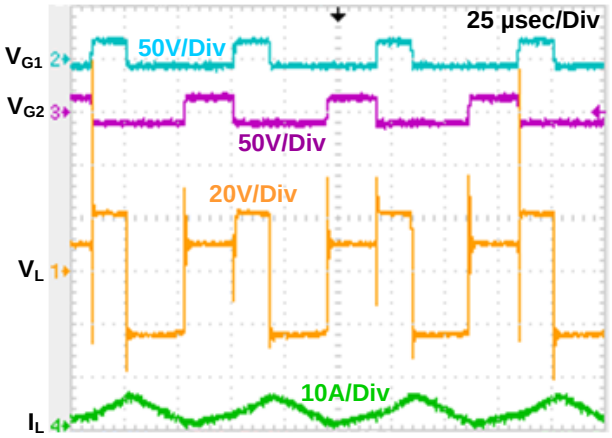

(a)

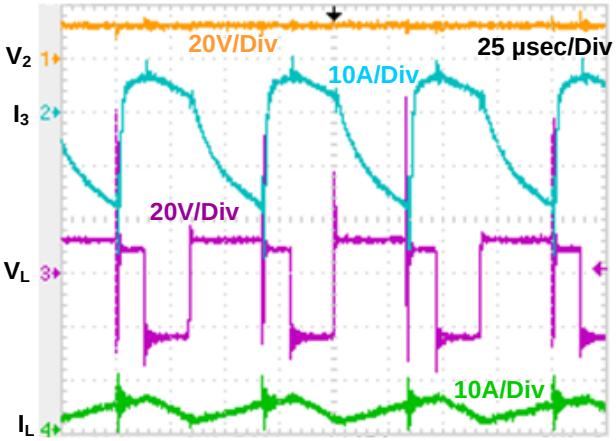

(b)

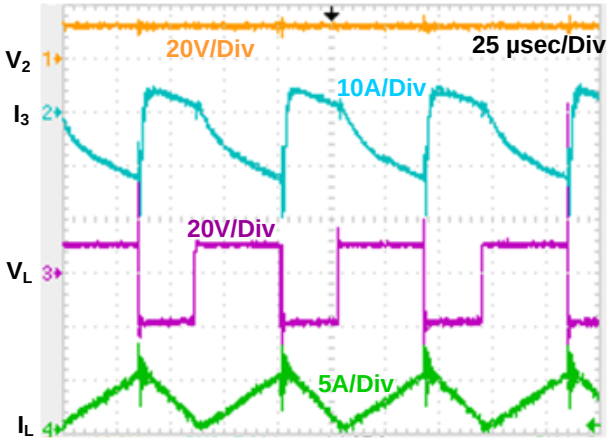

(c)

Figure 8: Experimental results: (a) Buck-boost mode of operation in steady state, (b) Charging of V_2 by V_1 when both V_1 and V_2 are active, (c) Charging of V_2 by V_1 when V_1 is acting alone

As V_2 dropped below specified value, gate pulse is applied to switch S_3, during the conduction period of S_1. The direction of current i_3 get reversed, as it flows through S_3 and D_2, as seen in Figure 8 (b). Figure 8 (b) show waveforms of MIC when V_1, V_2 are delivering power to the load at the same time V_2 is charged by V_1 during the OFF state of S_2. Negative value of i_3 shows charging of source V_2, whereas its positive value shows freewheeling of i_L. The voltage source V_1 charges source V_2 and inductor L. Thus, the MIC recharges ESS V_2.

When switch s_2 is on, V_2 supplies energy to inductor L. when s_2 is off and terminal voltage of V_2 falls below its rated value, source V_1 charges V_2, if s_3 is on. figure 8 (c) demonstrate charging of source V_2 when V_1 is acting alone.

CONCLUSIONS

In this paper, a flexible and reliable MIC for HES is proposed. Following are the salient features of the proposed MIC: it has the ability to supply energy from asymmetrical sources independently to the load; it is capable of transferring energy from one of the sources to the ESS; it maintains or recharges ESS during the operation of the converter, leading to improved reliability; output voltage is regulated at desired level during transient conditions of load as well as source; no dedicated converter is required for charging ESS, leading to enhanced utilization of the MIC; charging of the ESS is enhanced as less number of switches are present in the charging path; comparatively less part count as shown in Table 2; input sources and the load are isolated in all the states of operation without using transformer; and simple control.

Batteries or UCs are used as ESS, whereas charging source can be a renewable energy (solar) source. The usefulness and feasibility of the MIC is verified by performing detailed simulation and experimental studies. Steady and dynamic performance of the MIC is satisfactory. Experimental results of the converter proved that it is suitable in the applications of hybrid electric or renewable energy systems.

REFERENCES

[1] S. Danyali, S. H. Hosseini, G. B. Gharehpetian. “New extendable single stage multi-input dc–dc/ac boost converter”, IEEE Trans Power Electron., vol. 29(2), pp. 775-788, 2014.

[2] C. N. Onwuchekwa, A. Kwasinski. “A modified time sharing switching technique for multiple-input dc-dc converters”, IEEE Trans Power Electron., vol. 27(11), pp. 4492-4502, 2012.

[3] W. Jiang, B. Fahimi. “Multiport power electronic interface—concept, modeling, and design”, IEEE Trans Power Electron., vol. 26(7), pp. 1890-1900, 2011.

[4] L. Kumar, S. Jain. “Multiple-input dc/dc converter topology for hybrid energy system”, IET Power Electron., vol. 6(8), pp. 1483-1501, 2013.

[5] F. Liu, Z. Wang, Y. Mao, X. Ruan. “Asymmetrical half-bridge double-input dc/dc converters adopting pulsating voltage source cells for low power applications”, IEEE Trans Power Electron., vol. 29(9), pp. 4741- 4751, 2014.

[6] S. Dusmez, X. Li, B. Akin. “A new multiinput three-level dc/dc converter”, IEEE Trans Power Electron., vol. 31(2), pp. 1230-1240, 2016.

[7] W. Li, C. Xu, H. Luo, Y. Hu Y, X. He, C. Xia. “Decoupling-controlled triport composited dc/dc converter for multiple energy interface”, IEEE Trans Ind Electron., vol. 62(7), pp. 4504-4513, 2015.

[8] M. Sechilariu, B. Wang, F. Locment. “Building integrated photovoltaic system with energy storage and smart grid communication”, IEEE Trans Ind Electron., vol. 60(4), pp. 1607-1618, 2013.

[9] J. Zeng, W. Qiao, L. Qu, Y. Jiao. “An isolated multiport dc-dc converter for simultaneous power management of multiple different renewable energy sources”, IEEE J Emerg Select Topics Power Electron., vol. 2(1), pp. 70-78, 2014.

[10] M. Veerachary. “Multi-input integrated buck-boost converter for photovoltaic applications”, Proc. IEEE Inter Conf on Sustain Energ Technol., pp. 546–551, 2008.

[11] Y. Yuan-mao, K. W. E. Cheng. “Multi-input voltage-summation converter based on switched-capacitor”, IET Power Electron., vol. 6(9), pp. 1909–1916, 2013.

[12] H. Wu, J. Zhang, Y. Xing. “A family of multi-port buck-boost converters based on dc link inductors (DLIs)”, IEEE Trans Power Electron., vol. 30(2), pp. 735–746, 2015.

[13] R. Ahmadi, M. Ferdowsi. “Double-input converters based on h-bridge cells: derivation, small-signal modeling, and power sharing analysis”, IEEE Trans circuits syst., vol. 59(4), pp. 875-888, 2012.

[14] Y. Zheng, et al. “Electric vehicle battery charging/swap stations in distribution systems: comparison study and optimal planning”, IEEE Trans Power Syst., vol. 29(1), pp. 221-229, 2014.

[15] J. Hong, H. Lee, K. Nam. “Charging method for the secondary battery in dual-inverter drive systems for electric vehicles”, IEEE Trans Power Electron., vol. 30(2), pp. 909-921, 2015.

[16] M. Tabari, A. Yazdani. “A mathematical model for stability analysis of a dc distribution system for power system integration of plug-in electric vehicles”, IEEE Trans Veh Technol., vol. 64(5), pp. 1729-1738, 2014.